Specialty Journal of Pharmacognosy, Phytochemistry, and Biotechnology
ISSN: 3062-441X
2024, Volume 4, Page No: 104-117

Available online at: www.galaxypub.co/page/journals

Galaxy Publication

Galaxy Publication

A Novel Eight-lncRNA Disulfidptosis Signature Stratifies Prognosis and Immunotherapeutic Benefit in LUAD

Thandeka Moyo[1], Sipho Dlamini[1]*, Kabelo Ndlovu[1]

[1]Department of Pharmacognosy, Faculty of Health Sciences, University of Zimbabwe, Harare, Zimbabwe.

***E-mail** ✉ sipho.dlamini.pg@gmail.com

Received: 09 November 2023; **Revised:** 16 February 2024; **Accepted:** 19 February 2024

ABSTRACT

Lung adenocarcinoma (LUAD), the predominant form of lung malignancy, is associated with unfavorable clinical outcomes. Disulfidptosis, a recently described programmed cell-death mechanism, arises from excessive disulfide accumulation and disruption of the actin cytoskeleton. This work sought to pinpoint lncRNAs linked to disulfidptosis and to construct a disulfidptosis-associated lncRNA signature capable of forecasting LUAD prognosis and therapeutic responsiveness. RNA-seq profiles and clinical characteristics for LUAD cases were extracted from the TCGA database. Disulfidptosis-related lncRNAs connected to overall survival were screened through Pearson correlation together with Cox regression. A prognostic signature was produced via LASSO analysis. GO, KEGG, and GSEA functional annotations were applied to determine biological pathways enriched in the model. Immune infiltration was quantified using ESTIMATE and CIBERSORT. Simple nucleotide variation data were utilized to evaluate tumor mutational burden (TMB) and its relationship to the risk score. Patients' sensitivity to immunotherapy and antitumor agents was estimated via the TIDE algorithm and the GDSC platform.

A total of 127 lncRNAs associated with disulfidptosis were identified, and a prognostic panel containing eight of them (KTN1-AS1, AL365181.3, MANCR, LINC01352, AC090559.1, AC093673.1, AP001094.3, MHENCR) was constructed and validated. This model separated LUAD individuals into two distinct risk categories. Elevated risk scores independently predicted unfavorable overall survival and were linked to diminished immune infiltration, increased TMB, and weaker antitumor immune activation. High-risk cases were more likely to derive benefit from immune checkpoint blockade, whereas low-risk counterparts showed higher predicted responsiveness to targeted agents and multiple kinase inhibitors. We developed a disulfidptosis-associated lncRNA signature that may aid in forecasting survival, mutation burden, immune infiltration patterns, and likely responses to immunotherapy and targeted treatment in LUAD.

Keywords: Lung adenocarcinoma, Disulfidptosis, lncRNA, Prognosis, Immunotherapy

How to Cite This Article: Moyo T, Dlamini S, Ndlovu K. A Novel Eight-lncRNA Disulfidptosis Signature Stratifies Prognosis and Immunotherapeutic Benefit in LUAD. Spec J Pharmacogn Phytochem Biotechnol. 2024;4:104-17. https://doi.org/10.51847/ynKIf1yzPT

Introduction

Lung cancer continues to rank among the most common and lethal malignancies worldwide [1, 2]. Adenocarcinoma represents the predominant subtype of non-small cell lung cancer (NSCLC), making up roughly 40% of diagnosed lung tumors [3]. Early recognition is critical for therapeutic success, and delays often eliminate the best treatment window. For stage I–II disease, surgery is the primary approach. In advanced NSCLC, systemic options—including targeted agents and immune-based treatments—can supplement radiotherapy and chemotherapy depending on genomic alterations (such as EGFR mutations and ALK rearrangements) and PD-L1 expression levels [3]. LUAD demonstrates extensive molecular and phenotypic heterogeneity, with nearly 60% carrying at least one driver mutation, many of which correlate with clinical characteristics and treatment outcomes [4, 5]. Among these, KRAS and KEAP1 are frequently altered. In KRAS-mutant LUAD, KEAP1 mutations are associated with markedly reduced overall survival under anti-PD-(L)1 therapy (median OS (95% CI): 4.8 months

(4.0–8.0) for KEAP1-mutant vs. 18.4 months (14.9–221.7) for wild-type), an effect absent in KRAS wild-type disease [6]. Another LUAD cohort treated with immune checkpoint inhibitors demonstrated that KEAP1 loss-of-function—through somatic mutations and loss of heterozygosity—relates to poorer outcomes and an immune-excluded phenotype [7]. Despite progress in molecular diagnostics and targeted strategies, survival rates remain unsatisfactory [8]. A deeper understanding of LUAD-related molecular mechanisms is therefore essential for improving disease management.

Resisting regulated cell death is recognized as a core cancer characteristic [9]. A rapidly expanding body of work indicates that multiple regulated cell death modalities influence tumor behavior and treatment outcomes [10]. Ferroptosis, for instance—defined by iron-driven accumulation of lipid hydroperoxides—has been linked to T-cell–dependent antitumor immunity and contributes to the impact of immunotherapies [11]. Disulfidptosis, a newly delineated form of regulated cell death, arises when intracellular disulfides accumulate excessively in SLC7A11-high cells experiencing glucose deprivation [12]. Elevated SLC7A11-dependent cystine transport combined with glucose shortage triggers pronounced disulfide stress, promoting abnormal disulfide crosslinking of actin-associated proteins, which ultimately drives actin fiber contraction and detachment from the plasma membrane [12]. Recent findings by Chen *et al*. suggest that disulfidptosis influences bladder cancer biology and therapeutic response [13]. Nevertheless, its contribution to LUAD development and patient prognosis is still unknown.

Long non-coding RNAs (lncRNAs) are transcripts exceeding 200 nucleotides that lack protein-coding capability. Genomic loci encoding lncRNAs constitute one of the most abundant functional categories within the non-coding genome [14]. They modulate gene expression and protein activity via interactions with nucleic acids and proteins alike [15–17]. Because of their regulatory involvement in pathological contexts, lncRNAs have been associated with numerous diseases. In LUAD, accumulating evidence shows that specific lncRNAs can accelerate tumor progression (such as UPLA1 and LINC00628), enhance immune escape (e.g., SChLAP1), and function as biomarkers or potential therapeutic targets [18–20].

In this project, we sought to characterize disulfidptosis-linked lncRNAs relevant to LUAD prognosis. We generated and validated a prognostic signature centered on these lncRNAs, demonstrating strong predictive performance for survival (AUC for 1-year survival: 0.703). Furthermore, the risk score derived from the signature enabled assessment of immune microenvironment features as well as predicted sensitivity to immunotherapies and chemotherapeutic agents. Apart from tumor stage, the risk score served as an independent prognostic indicator capable of distinguishing high-risk cases (HR: 1.245, 95% CI: 1.167–1.328, $p < 0.001$). These results highlight crucial regulatory contributions of disulfidptosis-associated lncRNAs to LUAD and point toward possible therapeutic intervention strategies.

Materials and Methods

Data acquisition

RNA-seq–based transcriptomic data, clinical characteristics, and somatic mutation information for over 500 LUAD patients were obtained from the TCGA dataset. Normal controls were excluded prior to downstream processing. LUAD samples lacking essential details such as survival time, age, or tumor stage were also removed.

Screening for disulfidptosis-related lncRNAs

A panel of 25 disulfidptosis-associated genes was collected from earlier literature [12, 21, 22]. Pearson correlation analysis was then applied to pinpoint lncRNAs co-expressed with these genes, using $|\text{correlation coefficient}| > 0.4$ and $p < 0.001$ as filtering conditions. lncRNAs meeting these criteria were defined as disulfidptosis-related.

Establishment and validation of a disulfidptosis-related lncRNA prognostic model

A total of 507 LUAD cases with survival records were randomly split into a training cohort (n = 254) and a testing cohort (n = 253). Within the training cohort, univariate Cox regression was used to identify survival-associated disulfidptosis-related lncRNAs. After applying LASSO to select lncRNAs with minimal model penalty, eight lncRNAs were incorporated into a multivariate Cox-based prognostic model. The risk score was computed as the weighted sum of each lncRNA's expression and its regression coefficient, risk score = $\sum_{i=0}^{n} (\beta_i \times Exp_i)$ [23]. Patients were divided into high- and low-risk groups according to the median score, and overall survival was compared to assess prognostic effectiveness. The testing cohort was used to verify model stability. Multivariate

Cox regression was also performed to determine whether the model-derived risk score functions as an independent predictor for LUAD outcomes.

Functional enrichment analysis of differentially expressed genes

To distinguish transcriptomic differences between the two risk categories, we identified differentially expressed genes (DEGs) using the cutoffs |log2 fold change| > 1 and FDR < 0.05. After compiling the DEG list, we performed Gene Ontology (GO) and Kyoto Encyclopedia of Genes and Genomes (KEGG) enrichment analyses to reveal biological distinctions separating high- and low-risk groups. Any GO term or KEGG pathway with an FDR < 0.05 was regarded as significantly enriched. We additionally applied gene set enrichment analysis (GSEA) using GO gene sets to compare global expression patterns; enrichment was assigned when the p-value < 0.05 and FDR < 0.25.

Tumor-infiltrating immune cells analysis

The ESTIMATE algorithm [24] was utilized to infer stromal and immune cell levels in LUAD specimens based on expression data. It produces three indices—stromal, immune, and estimate scores—derived through single-sample GSEA, and these scores were contrasted between the high- and low-risk categories. To obtain a more detailed immune landscape, we applied the CIBERSORT approach [25], which quantifies 22 immune cell populations per sample. Immune-related signatures were also evaluated via single-sample GSEA, and differences in the activity of these immune functions were assessed across the two risk groups.

Tumor mutational burden analysis

Tumor mutational burden (TMB) and mutation rates for each patient were computed by counting all somatic base substitutions. TMB levels were then compared between high- and low-risk groups. By splitting patients at the median TMB, we conducted survival analyses to determine its effect on overall survival. We also examined how TMB interacts with the risk score to shape prognosis.

Immunotherapy response and drug sensitivity prediction

To predict the likelihood of response to anti-PD-1 and anti-CTLA4 therapies, we used the TIDE framework [26]. Since lower TIDE scores correspond to greater expected benefit from immunotherapy, we compared TIDE outputs between the two risk groups. Drug-response prediction was carried out using the oncoPredict R package, which leverages expression data and training models from the GDSC database. These models, obtained through oncoPredict's Open Science Framework (https://osf.io/c6tfx/) [27], were applied using the calcPhenotype function to derive sensitivity scores for each patient. These drug-specific scores were then compared across the two risk categories.

Statistical analysis

All computational work was performed using R (4.2.2). Evaluations of two-group differences were performed using two-tailed Student's t-tests. Kaplan–Meier curves with log-rank tests were used for survival assessment. A p-value < 0.05 was taken as the significance threshold unless stated otherwise.

Results and Discussion

Identification of disulfidptosis-related lncRNAs

LUAD RNA-seq data were obtained from TCGA, and transcripts were categorized into protein-coding mRNAs and lncRNAs based on genomic annotations. To identify lncRNAs connected to disulfidptosis, we conducted Pearson correlation analysis between all lncRNA expression profiles and a set of 25 disulfidptosis-associated genes. Using stringent criteria of |Pearson R| > 0.4 and p < 0.001, we identified 127 lncRNAs, each showing correlation with 20 out of the 25 disulfidptosis-related genes **(Figure 1a)**.

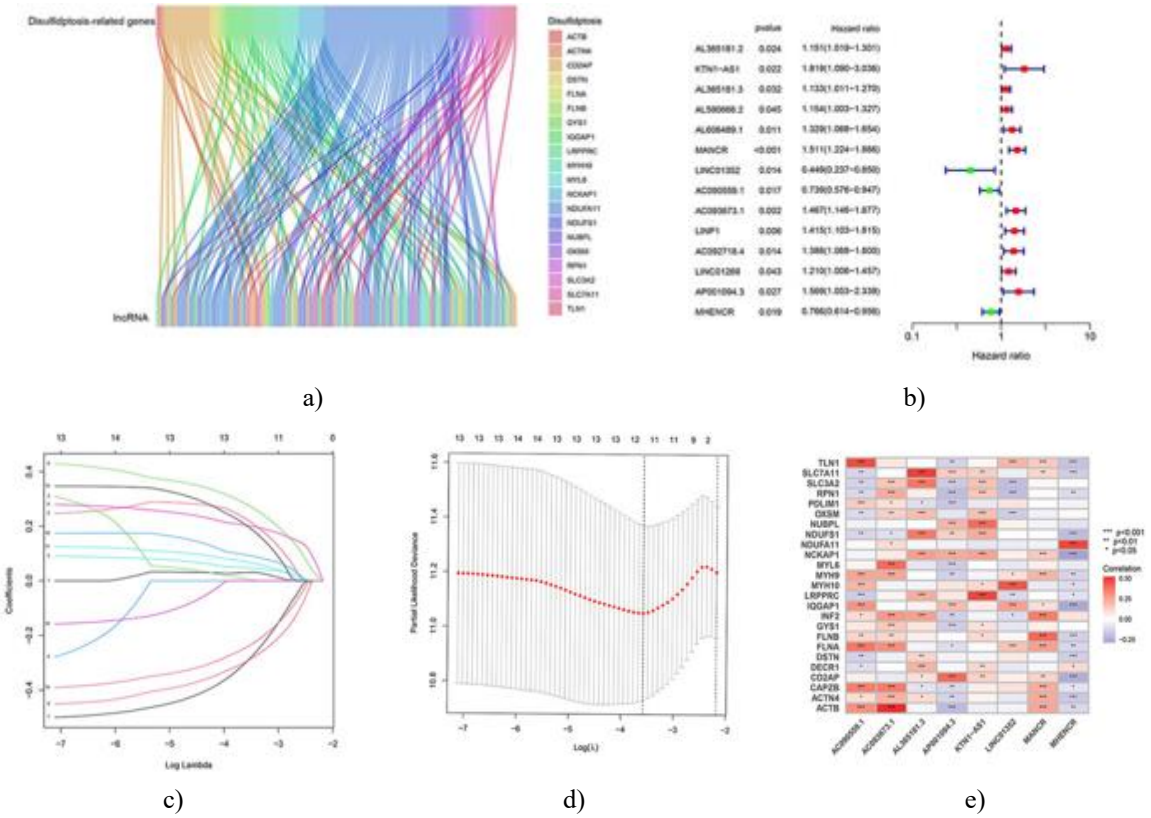

a) b) c) d) e)

Figure 1. Screening of lncRNAs related to disulfidptosis and development of a survival prediction model in LUAD.

(a) A Sankey plot illustrating significant expression associations between disulfidptosis-associated genes and 127 lncRNAs. (b) Univariate Cox regression identifies disulfidptosis-linked lncRNAs that influence overall survival in LUAD patients. (c) LASSO coefficient profiles for 14 survival-related lncRNAs. (d) LASSO cross-validation results; dashed lines mark the optimal log(λ). (e) Heatmap demonstrating the expression relationships between the eight model-selected lncRNAs and disulfidptosis-associated genes. *, $p < 0.05$; **, $p < 0.01$; ***, $p < 0.001$.

Construction of a prognostic model based on disulfidptosis-related lncRNAs

A total of 507 LUAD patients with available survival outcomes were randomly assigned into a training set for model formulation and a test set for validation. From the initial 127 lncRNAs, only those linked to patient prognosis were retained. Univariate Cox analysis eliminated lncRNAs without significant prognostic influence, leaving 14 associated lncRNAs. Among these, three were linked to better prognosis, and eleven were associated with poorer outcomes **(Figure 1b)**. Using these 14 survival-related lncRNAs, a LASSO Cox model incorporating 8 of them was generated **(Figures 1c and 1d)**. Each patient received a risk score calculated as follows:

risk score = (0.433 × KTN1-AS1 expression value (EV)) + (0.099 × AL365181.3 EV) + (0.274 × MANCR EV) − (0.604 × LINC01352 EV) − (0.404 × AC090559.1 EV) + (0.425 × AC093673.1 EV) + (0.374 × AP001094.3 EV) − (0.340 × MHENCR EV).

Figure 1e presents the correlations between the eight selected lncRNAs and 25 disulfidptosis-related genes. AC093673.1 and AL365181.3 demonstrated positive expression relationships with most targets, whereas AP001094.3 and MHENCR showed predominantly negative associations. Patients in the training cohort were separated into high- and low-risk groups based on the median risk score. As expected, individuals with higher scores showed shorter overall survival, confirming the predictive value of the eight-lncRNA panel **(Figure 2a)**. Comparable findings occurred within the test cohort and the combined dataset **(Figures 2b and 2c)**, supporting the robustness of the model. Additionally, expression trends of the eight lncRNAs relative to risk scores were consistent in both patient groups **(Figure 2d)**.

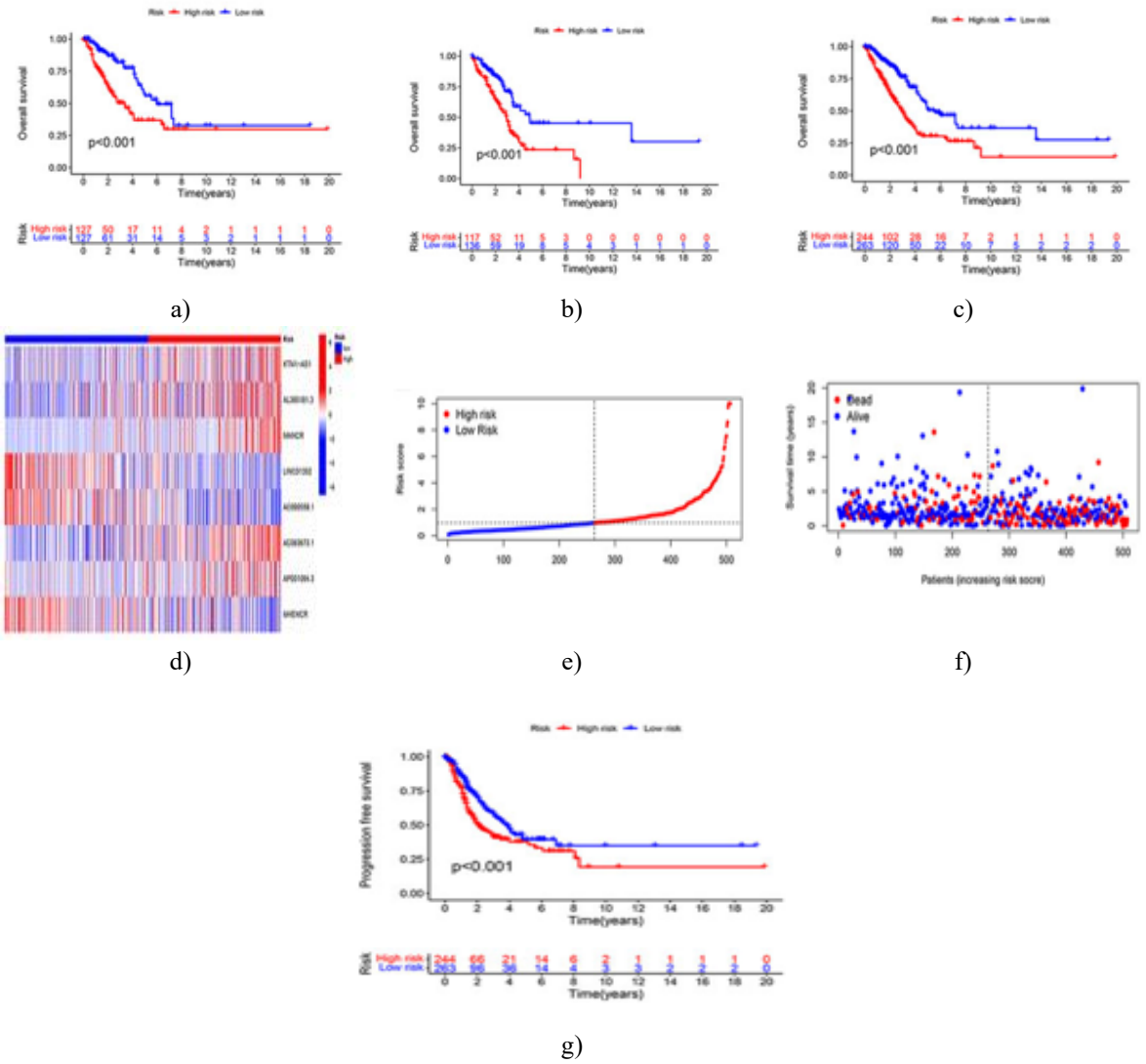

Figure 2. Validation and assessment of the prognostic significance of the disulfidptosis-lncRNA signature. (a, b) Kaplan–Meier curves showing differences in overall survival between low- and high-risk categories in the training (a) and test (b) datasets. (c, d) Kaplan–Meier curves illustrating differences in overall survival (c) and progression-free survival (d) in the merged LUAD cohort categorized by risk level. (e) Ordered distribution of patient risk scores. (f) Survival states of patients ranked by increasing risk score. (g) Heatmap comparing expression of the eight lncRNAs in high- versus low-risk patients.

After merging the two cohorts and re-stratifying them, each patient's score and outcome are displayed in **Figures 2e and 2f**. Higher risk scores corresponded to an increased likelihood of mortality. Additionally, elevated risk scores also signaled poorer progression-free survival **(Figure 2g)**.

The disulfidptosis-related lncRNA signature functions as an independent prognostic factor

To determine whether clinical characteristics influenced model performance, four LUAD clinical parameters—age, sex, tumor stage, and risk score—were evaluated via Cox regression. Univariate results showed that both tumor stage (HR: 1.639, 95% CI: 1.426–1.884, $p < 0.001$) and the eight-lncRNA risk score (HR: 1.225, 95% CI: 1.155–1.299, $p < 0.001$) were significant adverse predictors **(Figure 3a)**. Multivariate analysis further demonstrated that the risk score (HR: 1.245, 95% CI: 1.167–1.328, $p < 0.001$) and tumor stage (HR: 1.647, 95% CI: 1.428–1.900, $p < 0.001$) remained independent determinants of outcome **(Figure 3b)**. ROC analysis revealed AUC values of 0.703, 0.673, and 0.654 for 1-, 3-, and 5-year survival, confirming strong predictive accuracy **(Figure 3c)**. Notably, the prognostic performance of the model was close to that of tumor stage itself (AUCs: 0.673 vs. 0.687) **(Figure 3d)**. Overall, these results highlight that the disulfidptosis-associated lncRNA model provides a reliable and independent survival predictor.

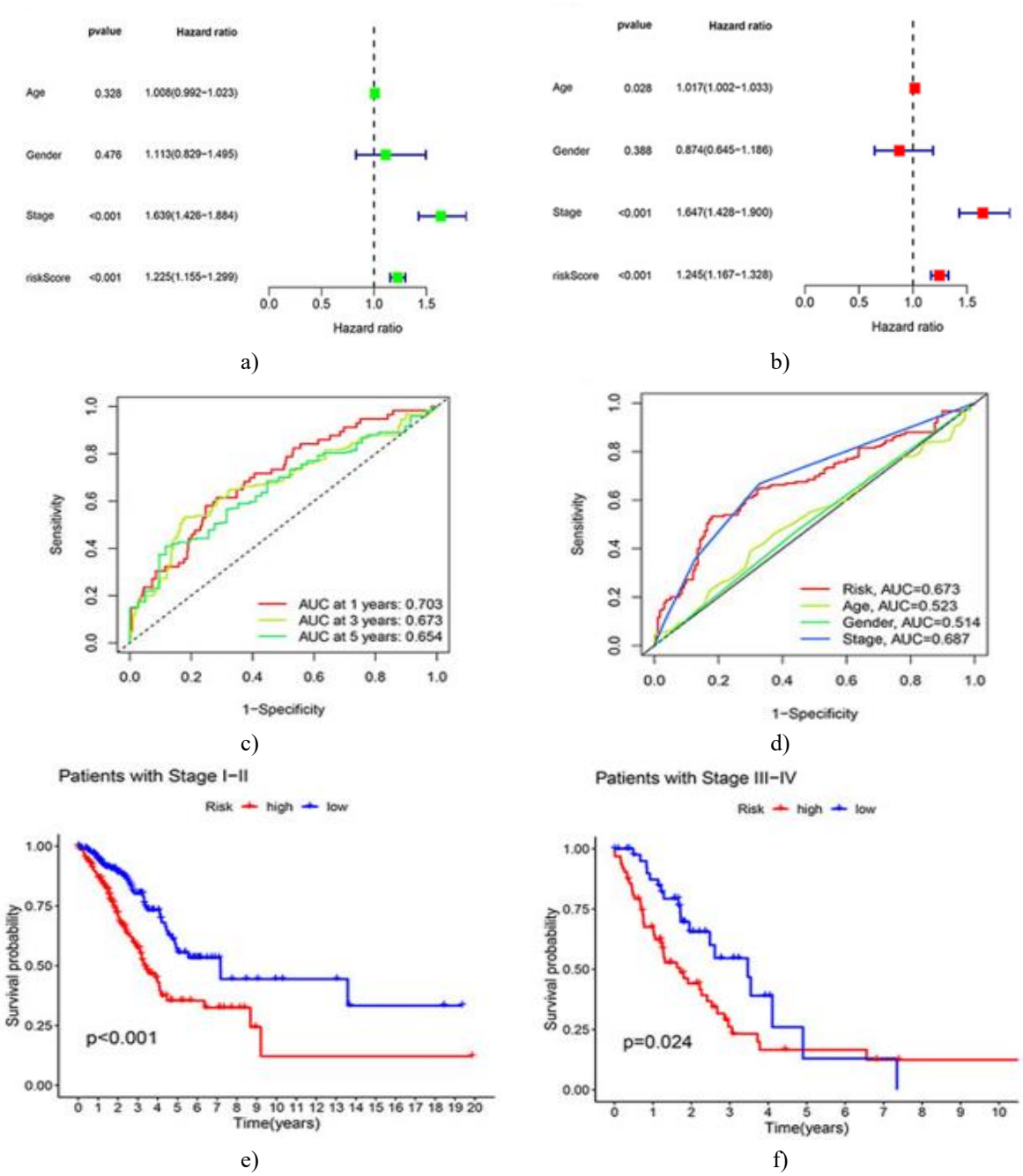

Figure 3. The eight-lncRNA disulfidptosis model serves as a highly accurate and independent prognostic factor.

(a) Forest chart illustrating the prognostic influence of age, sex, tumor stage, and risk score according to univariate Cox analysis. (b) Forest chart demonstrating that both tumor stage and the risk score derived from our model remain independent predictors in multivariate regression. (c) Predictive efficiency of the risk score in estimating 1-, 3-, and 5-year survival outcomes. (d) Comparative performance of risk score, stage, age, and gender in forecasting LUAD patient survival. (e, f) Kaplan–Meier curves presenting overall survival differences between high- and low-risk groups among early-stage patients (e) and advanced-stage patients (f).

Practical utility of the lncRNA model in patients at the same disease stage

Tumor stage and the constructed model both demonstrated strong predictive potential, leading us to evaluate how the model performs relative to staging alone. LUAD patients were stratified into early stages (I–II) and advanced stages (III–IV). Within both categories, individuals with elevated risk scores had significantly poorer overall survival compared with low-risk patients **(Figures 3e and 3f)**. Thus, the model can effectively distinguish risk levels among patients even when their tumor stages are the same.

Functional relevance of the disulfidptosis-related lncRNA profile in immune regulation

To uncover biological variations between high- and low-risk groups, differentially expressed gene (DEG) analysis was conducted, revealing 643 DEGs. GO analysis indicated associations with processes including microtubule-based movement, humoral immune activity, and ciliary motion **(Figure 4a)**. KEGG pathway mapping showed enrichment in systemic lupus erythematosus and neutrophil extracellular trap formation **(Figure 4b)**. In addition, GSEA using transcriptomic data revealed that nucleosome assembly, DNA packaging structures, protein-DNA complexes, and chromatin structural components were dominant in the high-risk group. Conversely, pathways such as B-cell receptor signaling, complement activation, immunoglobulin complexes, T-cell receptor complexes, and immunoglobulin-receptor binding were preferentially enriched in the low-risk group **(Figures 4c and 4d)**.

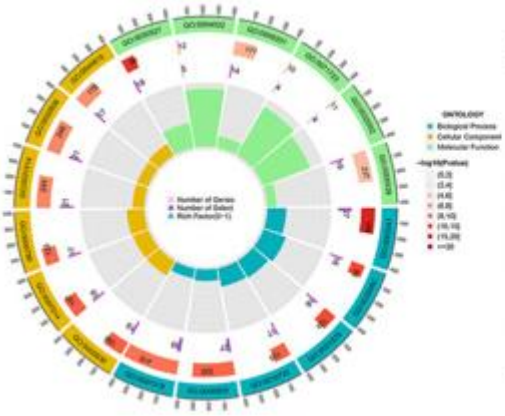

ID	Description
GO:0003341	cilium movement
GO:0035082	axoneme assembly
GO:0001578	microtubule bundle formation
GO:0019730	antimicrobial humoral response
GO:0006959	humoral immune response
GO:0007018	microtubule-based movement
GO:0005930	axoneme
GO:0097014	ciliary plasm
GO:0000786	nucleosome
GO:0031514	motile cilium
GO:0032838	plasma membrane bounded cell projection cytoplasm
GO:0044815	DNA packaging complex
GO:0030527	structural constituent of chromatin
GO:0004032	alditol:NADP+ 1-oxidoreductase activity
GO:0008201	heparin binding
GO:0071723	lipopeptide binding

a)

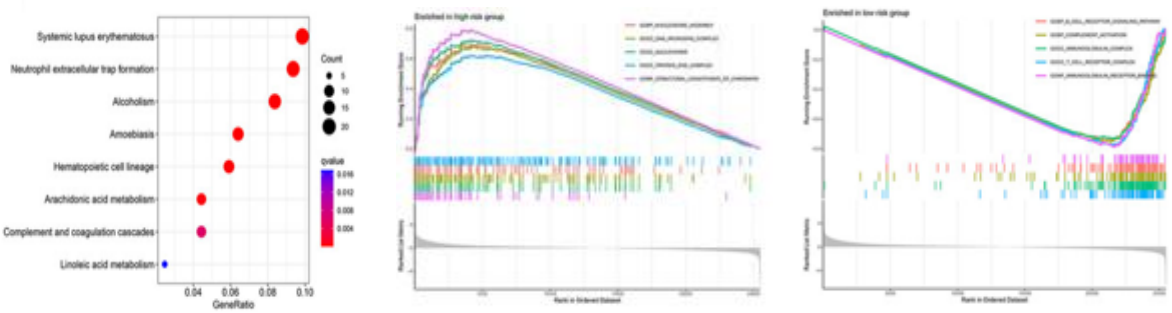

b) c) d)

Figure 4. Functional enrichment differences between LUAD patients classified as high or low risk. (a, b) GO (a) and KEGG (b) analyses of DEGs between the two groups. (c, d) GSEA results highlighting enriched processes in high-risk LUAD (c) and low-risk LUAD (d).

Given the critical role of the tumor immune microenvironment in cancer progression, and considering that GSEA pointed to immune enrichment in low-risk patients, we examined immune differences between groups. Based on ESTIMATE, immune scores were markedly lower in the high-risk cohort **(Figure 5a)**, suggesting reduced immune cell presence. CIBERSORT analysis further revealed that high-risk tumors contained fewer monocytes, resting dendritic cells, and resting mast cells, while showing increased M0 macrophage infiltration **(Figure 5b)**. Examination of immune functions demonstrated that 25 of 29 immune activities—such as B-cell involvement, CD8+ T-cell response, and cytolytic potential—were significantly weaker in high-risk LUAD cases compared with low-risk patients **(Figure 5c)**. Overall, these findings imply that high-risk tumors defined by the eight-lncRNA model may exhibit impaired antitumor immunity, contributing to disease advancement and reduced survival.

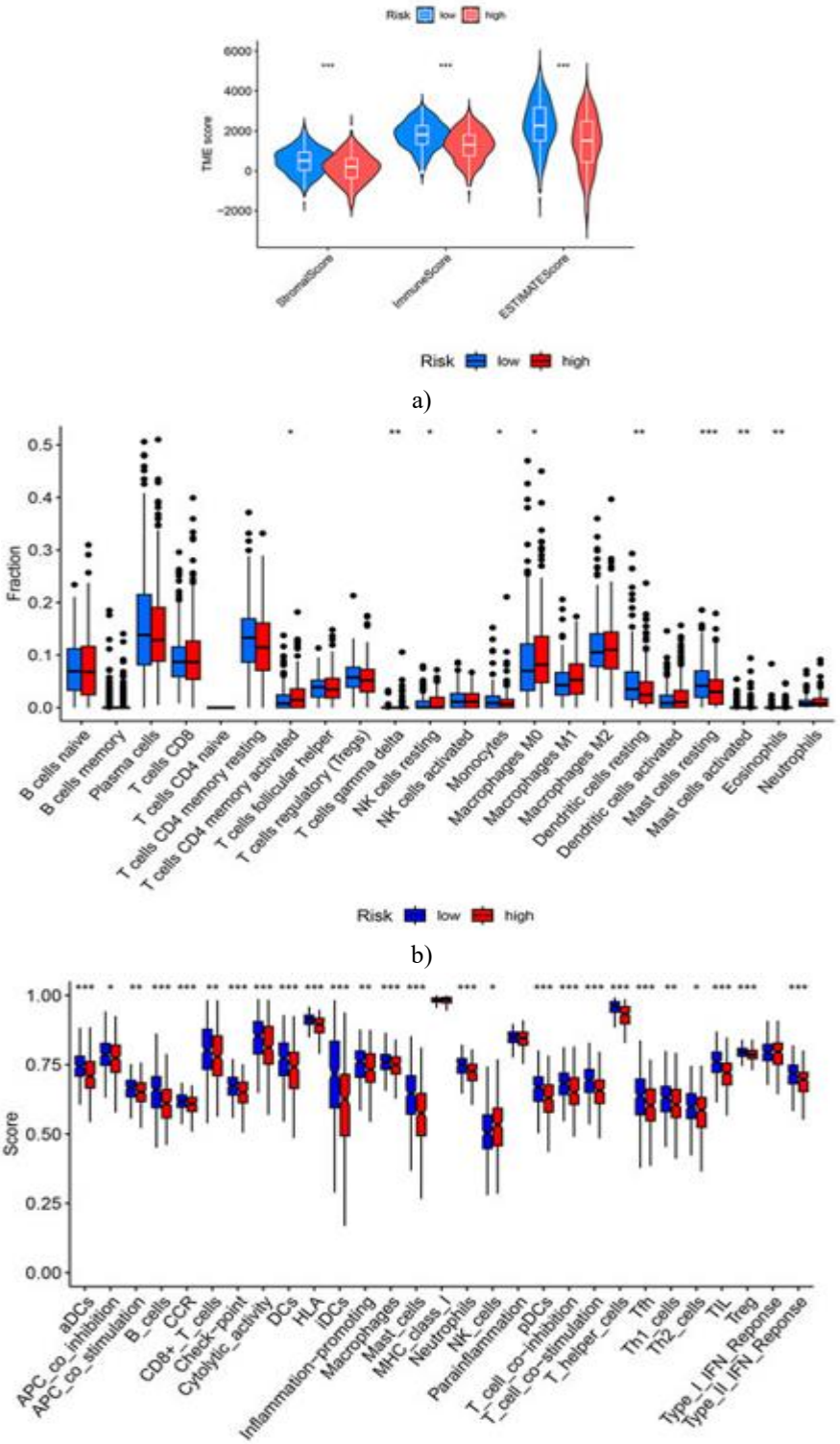

a)

b)

c)

Figure 5. Distinct immune infiltration signatures in high- versus low-risk LUAD.
(a) Violin plots showing stromal and immune score differences between groups. (b) Comparison of infiltration levels for 22 immune cell types within the tumor microenvironment. (c) Differences in 29 immune functional categories between high- and low-risk cases. *, $p < 0.05$; **, $p < 0.01$; ***, $p < 0.001$.

Mutational characteristics of LUAD subgroups defined by the disulfidptosis-related lncRNA signature

Tumor mutational burden (TMB)—referring to the total number of somatic variants per megabase—is widely regarded as a predictive biomarker in multiple cancers [28]. We compared TMB levels and mutation profiles between the two LUAD subgroups. High-risk tumors showed notably elevated TMB relative to low-risk tumors

(Figure 6a). TMB scores for individual samples and the 20 genes with the highest mutation prevalence, along with mutation categories, are presented in **Figures 6b and 6c**. Nearly all of these genes demonstrated higher mutation rates in high-risk cases, with TP53 and TTN altered in over 50% of this subgroup. Elevated TMB was associated with improved survival, as patients with high TMB had significantly better overall outcomes compared with those with low TMB **(Figure 6d)**. We further assessed the combined impact of TMB classification and model-derived risk score by dividing patients into four categories. Individuals with high TMB and low risk scores had the most favorable outcomes, with a 10-year survival close to 60%. Conversely, those with low TMB and high risk scores showed the worst results, with only about 25% surviving beyond five years. Patients classified as high TMB/high risk or low TMB/low risk demonstrated intermediate outcomes without significant differences between the two groups **(Figure 6e)**.

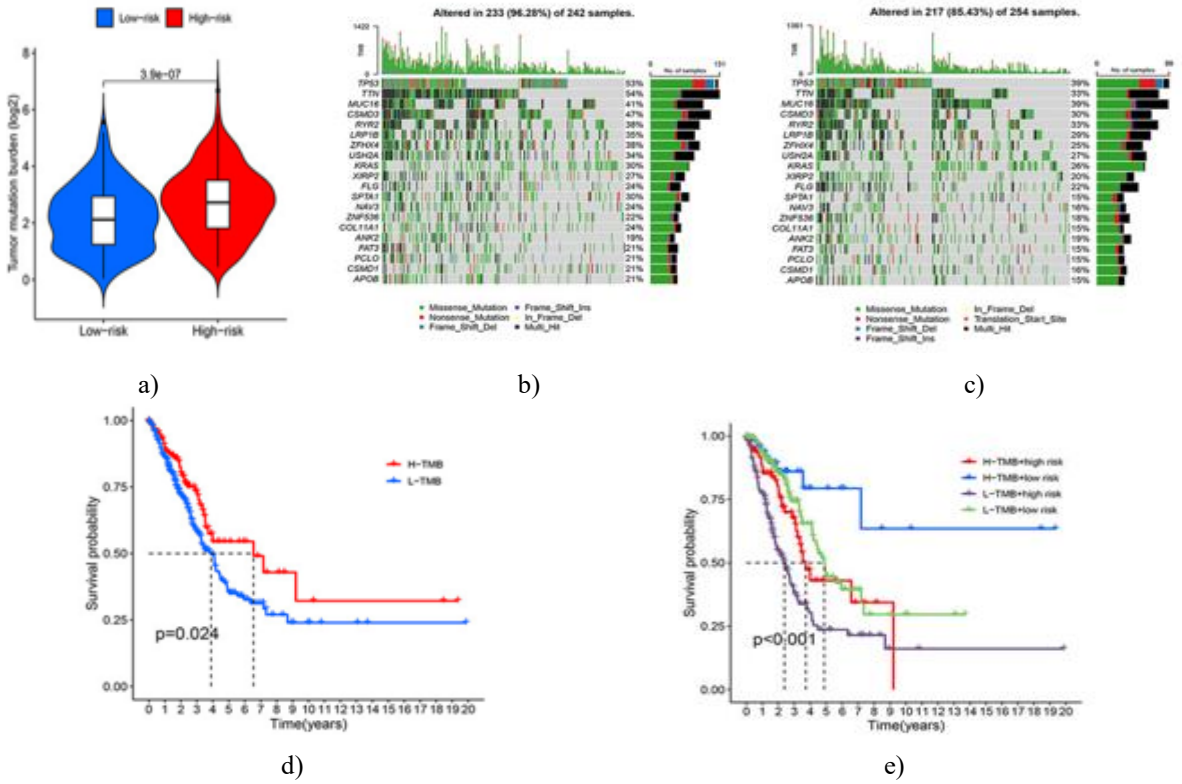

Figure 6. Variations in TMB and somatic mutation frequency between LUAD high- and low-risk groups. (a) Violin plot with embedded boxplot comparing overall TMB between the two groups. (b, c) Waterfall plots illustrating mutation rates of the top 20 most frequently altered genes in high-risk (b) and low-risk (c) LUAD samples. The upper histograms display TMB per sample, while different mutation types are color-coded, with right-side histograms showing the number of samples harboring each mutation type. (d) Kaplan–Meier curves depicting survival differences between high- and low-TMB patients. (e) Kaplan–Meier analysis of patient outcomes across four combined TMB–risk subgroups defined by the lncRNA model.

Forecasting susceptibility to immunotherapy and additional anticancer agents

Therapy resistance is a major factor contributing to recurrence and mortality in oncology. Immune checkpoint blockade (ICB) has shown substantial benefit in selected NSCLC cases. To examine whether the disulfidptosis-lncRNA model could help identify LUAD patients likely to benefit from immunotherapy, we assessed correlations between the model-based risk score and TIDE values. High-risk patients exhibited significantly reduced TIDE scores **(Figure 7a)**, indicating that they may respond more favorably to ICB treatment. Given that our findings also showed elevated TMB in high-risk tumors **(Figure 6a)**, these results are consistent with previous evidence linking high TMB to improved outcomes following PD-1 inhibition [29].

We also evaluated how the model-related risk score corresponds to predicted sensitivity to common anticancer drugs. Drug response values were calculated using the calcPhenotype function in the oncoPredict workflow from patient gene expression data and reference datasets. Compared with the low-risk subset, high-risk patients showed reduced predicted sensitivity to multiple targeted therapies, including:

- EGFR tyrosine kinase inhibitors: gefitinib, erlotinib, AZD3759 **(Figure 7b)**
- MEK/ERK pathway inhibitors: Trametinib, PD0325901, Ulixertinib, ERK_6604 **(Figure 7c)**
- Cell cycle-associated kinase inhibitors: AZD7762, BI-2536, MK-1775 **(Figure 7d)**
- MET inhibitors: Savolitinib, Foretinib, Crizotinib **(Figure 7e)**
- DNA integrity–disrupting drugs: Talazoparib, AZD6738, VE821, GDC0810 **(Figure 7f)**

These observations support that the disulfidptosis-related lncRNA signature may assist in forecasting patient response to both ICB and commonly used chemotherapeutic and targeted agents.

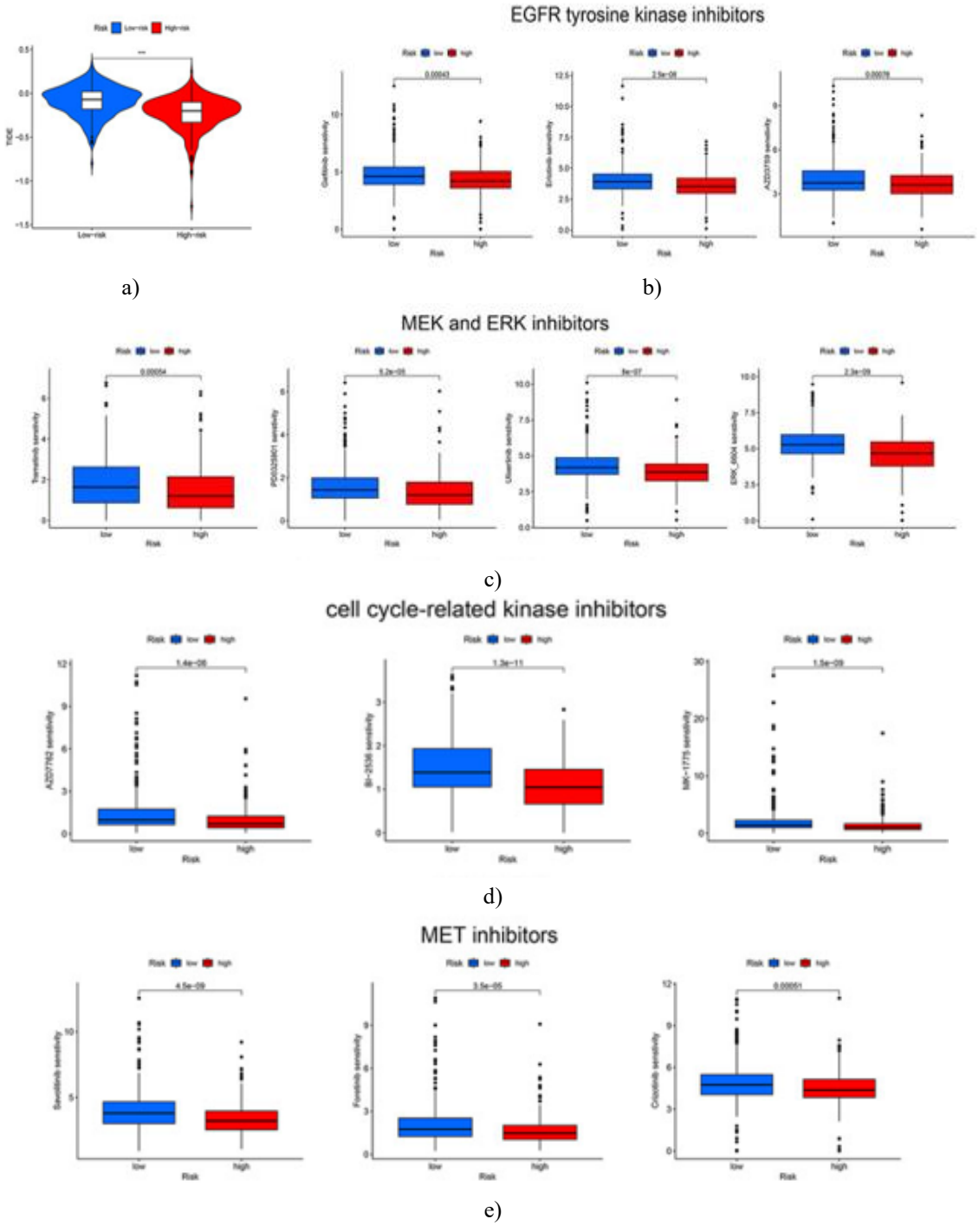

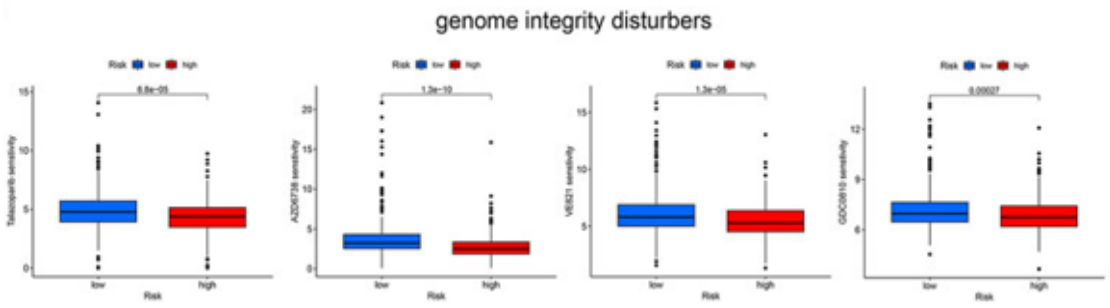

f)

Figure 7. Estimated treatment responses in the two LUAD risk subgroups to ICB and additional antitumor medications.

(a) Violin plot depicting differences in TIDE scores between high- and low-risk tumors. (b–e) Comparison of the two groups' predicted sensitivity to kinase inhibitors, including EGFR-targeting drugs (b), MEK/ERK inhibitors (c), cell cycle kinase inhibitors (d), and MET inhibitors (e). (f) Differences in predicted responses to agents affecting genome stability. ***, $p < 0.001$.

Disulfidptosis is defined as a cell death mechanism triggered by excessive cystine accumulation and depletion of NADPH, which results in improper disulfide cross-linking among actin cytoskeleton proteins and eventual collapse of the actin framework [12]. Because tumor cells are especially susceptible to this process, exploiting disulfidptosis has been proposed as a novel treatment approach in oncology. Signatures based on disulfidptosis have already been applied to forecast outcomes in several cancers, such as hepatocellular carcinoma and bladder cancer [13, 30]. Long noncoding RNAs are crucial regulators of cancer progression and have been widely reported as diagnostic and therapeutic biomarkers [31]. However, lncRNAs involved in disulfidptosis are still largely unexplored, and their prognostic relevance in LUAD has not been clarified. In this work, we identified lncRNAs correlated with disulfidptosis-related genes and developed an LUAD prognostic model composed of eight such lncRNAs.

We detected 127 lncRNAs associated with disulfidptosis, after which those linked to overall survival in LUAD were selected to construct the model. Using LASSO regression, we built a risk scoring system consisting of eight prognostic disulfidptosis-related lncRNAs. Its performance was validated in both the training and test datasets, which together included more than 500 LUAD cases. A higher risk score generated by the model predicted shorter progression-free and overall survival. Tumor stage is a well-acknowledged indicator reflecting tumor advancement and clinical severity. As anticipated, our findings confirmed that tumor stage served as an independent prognostic variable in LUAD. Likewise, the risk score derived from our lncRNA signature demonstrated standalone prognostic value and was comparable to tumor stage in forecasting 3- and 5-year survival. Importantly, unlike staging alone, the model can differentiate high- and low-risk patients who share the same clinical stage. Therefore, this disulfidptosis-related lncRNA classifier provides a dependable and precise tool for outcome prediction in LUAD.

The interactions between tumor cells and immune components in the microenvironment significantly influence cancer development. The prevalence and function of infiltrating immune cells are recognized predictors of clinical outcomes and treatment responses across many malignancies, including oral squamous cell carcinoma, HER2-enriched breast cancer, and epithelial ovarian carcinoma [32–35]. In our analysis, LUAD patients with high and low risk scores exhibited distinct levels of immune infiltration and immune-associated activity. Elevated risk scores showed strong negative correlations with pathways involving the T cell receptor complex, B cell receptor signaling, and immunoglobulin formation. T cell receptors are essential for tumor antigen recognition and the activation of T cell–mediated antitumor responses [36], while B cells contribute to humoral immunity and may suppress tumor progression through antibody secretion [37]. These observations point to weakened antitumor immunity in high-risk tumors. Furthermore, ESTIMATE analysis revealed that high-risk LUAD presented lower immune scores, indicating fewer immune cells occupying the tumor niche. Except for NK cells, which demonstrated slightly higher activity, most immune cell types—such as CD8+ T cells, macrophages, Dendritic cells, and B cells—displayed substantially reduced functional scores in the high-risk group. Collectively, the data suggest that diminished immune infiltration and immune response capacity likely contribute to the poorer

prognosis of high-risk LUAD patients, and these individuals can be effectively stratified using our disulfidptosis-associated lncRNA model.

Despite immune checkpoint inhibitors offering notable survival improvements in NSCLC, only a limited subset of patients shows a positive clinical response [38, 39]. Therefore, we examined whether the disulfidptosis-associated lncRNA signature could be applied to estimate treatment response to immune checkpoint blockade (ICB) in LUAD. Our results demonstrated that individuals categorized as high-risk exhibited reduced TIDE scores, implying a greater likelihood of benefiting from ICB therapy. This observation may be linked to the higher TMB seen in these patients, as elevated TMB has been regarded as a marker for improved immunotherapy effectiveness [29, 40]. Conversely, high-risk cases appeared less responsive to additional anticancer strategies, including EGFR tyrosine kinase inhibitors, MEK/ERK pathway inhibitors, MET-targeted drugs, and agents that interfere with genome maintenance or cell cycle progression.

Since somatic driver alterations play a key role in cancer initiation and advancement, and because high-risk LUADs showed higher TMB, we further assessed the genes most frequently mutated and compared the two patient risk groups. Among the 20 genes with the highest mutation incidence, 19 showed increased mutation rates in the high-risk cohort. Moreover, the high-risk group contained 10 genes with mutation frequencies of at least 30%, whereas the low-risk group contained only 5. TTN displayed the greatest mutation prevalence at 54% in high-risk LUAD and may contribute to elevated TMB, as TTN alterations are considered markers of high mutational burden [41]. Mutations in the tumor suppressor TP53, among the most widespread genetic events in cancer, were identified in 53% of high-risk cases. Additionally, oncogenic mutations, including those in MUC16 [42] and KRAS [43], were more common in the high-risk population, which may further explain their poorer outcomes beyond reduced immune infiltration and activity.

Conclusion

In summary, we identified disulfidptosis-related lncRNAs and used eight of them to develop and validate a prognostic model capable of independently predicting overall survival in LUAD patients, indicating immune characteristics of the tumor environment, and estimating the likelihood of response to immunotherapy, targeted agents, and chemotherapy. This work offers initial evidence linking disulfidptosis to immune responses in cancer. Nevertheless, certain limitations exist. Although the model's prognostic ability was confirmed in over 500 LUAD samples, the analysis relied exclusively on TCGA RNA-seq datasets. Validation with transcriptomic data from additional independent LUAD cohorts is necessary, and its applicability to results derived from other platforms remains unknown. Furthermore, although the eight lncRNAs correlate in expression with disulfidptosis-associated genes, their precise functions in regulating disulfidptosis have yet to be defined. The detailed molecular pathways through which these lncRNAs influence LUAD prognosis and therapeutic responses require further experimental investigation.

Acknowledgments: None

Conflict of Interest: None

Financial Support: None

Ethics Statement: None

References

1. Sung H, Ferlay J, Siegel RL, Laversanne M, Soerjomataram I, Jemal A, et al. Global cancer statistics 2020: GLOBOCAN estimates of incidence and mortality worldwide for 36 cancers in 185 countries. CA Cancer J Clin. 2021;71(3):209–49. doi:10.3322/caac.21660
2. Zheng JY, Zhu T, Zhuo W, Mao XY, Yin JY, Li X, et al. eIF3a sustains non-small cell lung cancer stem cell-like properties by promoting YY1-mediated transcriptional activation of beta-catenin. Biochem Pharmacol. 2023;213(1):115616. doi:10.1016/j.bcp.2023.115616
3. Duma N, Santana-Davila R, Molina JR. Non-small cell lung cancer: Epidemiology, screening, diagnosis, and treatment. Mayo Clin Proc. 2019;94(8):1623–40. doi:10.1016/j.mayocp.2019.01.013

4. Sholl LM. Biomarkers in lung adenocarcinoma: A decade of progress. Arch Pathol Lab Med. 2015;139(4):469–80. doi:10.5858/arpa.2014-0128-RA
5. Tavernari D, Battistello E, Dheilly E, Petruzzella AS, Mina M, Sordet-Dessimoz J, et al. Nongenetic evolution drives lung adenocarcinoma spatial heterogeneity and progression. Cancer Discov. 2021;11(6):1490–507. doi:10.1158/2159-8290.CD-20-1274
6. Ricciuti B, Arbour KC, Lin JJ, Vajdi A, Vokes N, Hong L, et al. Diminished efficacy of PD-(L)1 inhibition in STK11- and KEAP1-mutant lung adenocarcinoma is affected by KRAS mutation status. J Thorac Oncol. 2022;17(3):399–410. doi:10.1016/j.jtho.2021.10.013
7. Scalera S, Ricciuti B, Mazzotta M, Calonaci N, Alessi JV, Cipriani L, et al. Clonal KEAP1 mutations with loss of heterozygosity share reduced immunotherapy efficacy and low immune cell infiltration in lung adenocarcinoma. Ann Oncol. 2023;34(3):275–88. doi:10.1016/j.annonc.2022.12.002
8. Zhang C, Zhang J, Xu FP, Wang YG, Xie Z, Su J, et al. Genomic landscape and immune microenvironment features of preinvasive and early invasive lung adenocarcinoma. J Thorac Oncol. 2019;14(11):1912–23. doi:10.1016/j.jtho.2019.07.031
9. Hanahan D. Hallmarks of cancer: New dimensions. Cancer Discov. 2022;12(1):31–46. doi:10.1158/2159-8290.CD-21-1059
10. Peng F, Liao M, Qin R, Zhu S, Peng C, Fu L, et al. Regulated cell death (RCD) in cancer: Key pathways and targeted therapies. Signal Transduct Target Ther. 2022;7(1):286. doi:10.1038/s41392-022-01110-y
11. Wang W, Green M, Choi JE, Gijon M, Kennedy PD, Johnson JK, et al. $CD8^+$ T cells regulate tumour ferroptosis during cancer immunotherapy. Nature. 2019;569(7755):270–4. doi:10.1038/s41586-019-1170-y
12. Liu X, Nie L, Zhang Y, Yan Y, Wang C, Colic M, et al. Actin cytoskeleton vulnerability to disulfide stress mediates disulfidptosis. Nat Cell Biol. 2023;25(3):404–14. doi:10.1038/s41556-023-01091-2
13. Chen H, Yang W, Li Y, Ma L, Ji Z. Leveraging a disulfidptosis-based signature to improve the survival and drug sensitivity of bladder cancer patients. Front Immunol. 2023;14(1):1198878. doi:10.3389/fimmu.2023.1198878
14. Uszczynska-Ratajczak B, Lagarde J, Frankish A, Guigo R, Johnson R. Towards a complete map of the human long non-coding RNA transcriptome. Nat Rev Genet. 2018;19(9):535–48. doi:10.1038/s41576-018-0017-y
15. Liu B, Sun L, Liu Q, Gong C, Yao Y, Lv X, et al. A cytoplasmic NF-κB interacting long noncoding RNA blocks IκB phosphorylation and suppresses breast cancer metastasis. Cancer Cell. 2015;27(3):370–81. doi:10.1016/j.ccell.2015.02.004
16. Blank-Giwojna A, Postepska-Igielska A, Grummt I. lncRNA KHPS1 activates a poised enhancer by triplex-dependent recruitment of epigenomic regulators. Cell Rep. 2019;26(11):2904–15. doi:10.1016/j.celrep.2019.02.059
17. Statello L, Guo CJ, Chen LL, Huarte M. Gene regulation by long non-coding RNAs and its biological functions. Nat Rev Mol Cell Biol. 2021;22(2):96–118. doi:10.1038/s41580-020-00315-9
18. Xu SF, Zheng Y, Zhang L, Wang P, Niu CM, Wu T, et al. Long non-coding RNA LINC00628 interacts epigenetically with the LAMA3 promoter and contributes to lung adenocarcinoma. Mol Ther Nucleic Acids. 2019;18(1):166–82. doi:10.1016/j.omtn.2019.08.005
19. Han X, Jiang H, Qi J, Li J, Yang J, Tian Y, et al. Novel lncRNA UPLA1 mediates tumorigenesis and prognosis in lung adenocarcinoma. Cell Death Dis. 2020;11(11):999. doi:10.1038/s41419-020-03198-y
20. Du Z, Niu S, Wang J, Wu J, Li S, Yi X. SChLAP1 contributes to non-small cell lung cancer cell progression and immune evasion through regulating the AUF1/PD-L1 axis. Autoimmunity. 2021;54(4):225–33. doi:10.1080/08916934.2021.1913582
21. Yang L, Liu J, Li S, Liu X, Zheng F, Xu S, et al. Based on disulfidptosis, revealing the prognostic and immunological characteristics of renal cell carcinoma with tumor thrombus of vena cava and identifying potential therapeutic target AJAP1. J Cancer Res Clin Oncol. 2023;149(9):9787–804. doi:10.1007/s00432-023-04877-x
22. Zhao S, Wang L, Ding W, Ye B, Cheng C, Shao J, et al. Crosstalk of disulfidptosis-related subtypes, establishment of a prognostic signature and immune infiltration characteristics in bladder cancer based on a machine learning survival framework. Front Endocrinol (Lausanne). 2023;14(1):1180404. doi:10.3389/fendo.2023.1180404
23. Zhu T, Zheng J, Hu S, Zhang W, Zhou H, Li X, et al. Construction and validation of an immunity-related prognostic signature for breast cancer. Aging (Albany NY). 2020;12(21):21597–612. doi:10.18632/aging.103952

24. Yoshihara K, Shahmoradgoli M, Martinez E, Vegesna R, Kim H, Torres-Garcia W, et al. Inferring tumour purity and stromal and immune cell admixture from expression data. Nat Commun. 2013;4(1):2612. doi:10.1038/ncomms3612
25. Chen B, Khodadoust MS, Liu CL, Newman AM, Alizadeh AA. Profiling tumor infiltrating immune cells with CIBERSORT. Methods Mol Biol. 2018;1711(1):243–59. doi:10.1007/978-1-4939-7493-1_12
26. Jiang P, Gu S, Pan D, Fu J, Sahu A, Hu X, et al. Signatures of T cell dysfunction and exclusion predict cancer immunotherapy response. Nat Med. 2018;24(10):1550–8. doi:10.1038/s41591-018-0136-1
27. Maeser D, Gruener RF, Huang RS. oncoPredict: an R package for predicting in vivo or cancer patient drug response and biomarkers from cell line screening data. Brief Bioinform. 2021;22(6):bbab260. doi:10.1093/bib/bbab260
28. Sha D, Jin Z, Budczies J, Kluck K, Stenzinger A, Sinicrope FA. Tumor mutational burden as a predictive biomarker in solid tumors. Cancer Discov. 2020;10(12):1808–25. doi:10.1158/2159-8290.CD-20-0522
29. Rizvi NA, Hellmann MD, Snyder A, Kvistborg P, Makarov V, Havel JJ, et al. Mutational landscape determines sensitivity to PD-1 blockade in non-small cell lung cancer. Science. 2015;348(6230):124–8. doi:10.1126/science.aaa1348
30. Wang T, Guo K, Zhang D, Wang H, Yin J, Cui H, et al. Disulfidptosis classification of hepatocellular carcinoma reveals correlation with clinical prognosis and immune profile. Int Immunopharmacol. 2023;120(1):110368. doi:10.1016/j.intimp.2023.110368
31. Chi Y, Wang D, Wang J, Yu W, Yang J. Long non-coding RNA in the pathogenesis of cancers. Cells. 2019;8(9):1015. doi:10.3390/cells8091015
32. Salgado R, Denkert C, Campbell C, Savas P, Nuciforo P, Aura C, et al. Tumor-infiltrating lymphocytes and associations with pathological complete response and event-free survival in HER2-positive early-stage breast cancer treated with lapatinib and trastuzumab: A secondary analysis of the NeoALTTO trial. JAMA Oncol. 2015;1(4):448–54. doi:10.1001/jamaoncol.2015.0830
33. Hwang C, Lee SJ, Lee JH, Kim KH, Suh DS, Kwon BS, et al. Stromal tumor-infiltrating lymphocytes evaluated on H&E-stained slides are an independent prognostic factor in epithelial ovarian cancer and ovarian serous carcinoma. Oncol Lett. 2019;17(5):4557–65. doi:10.3892/ol.2019.10095
34. Shaban M, Khurram SA, Fraz MM, Alsubaie N, Masood I, Mushtaq S, et al. A novel digital score for abundance of tumour infiltrating lymphocytes predicts disease free survival in oral squamous cell carcinoma. Sci Rep. 2019;9(1):13341. doi:10.1038/s41598-019-49710-z
35. Paijens ST, Vledder A, de Bruyn M, Nijman HW. Tumor-infiltrating lymphocytes in the immunotherapy era. Cell Mol Immunol. 2021;18(4):842–59. doi:10.1038/s41423-020-00565-9
36. Zhong S, Malecek K, Johnson LA, Yu Z, Vega-Saenz de Miera E, Darvishian F, et al. T-cell receptor affinity and avidity defines antitumor response and autoimmunity in T-cell immunotherapy. Proc Natl Acad Sci U S A. 2013;110(17):6973–8. doi:10.1073/pnas.1221609110
37. Wang SS, Liu W, Ly D, Xu H, Qu L, Zhang L. Tumor-infiltrating B cells: Their role and application in anti-tumor immunity in lung cancer. Cell Mol Immunol. 2019;16(1):6–18. doi:10.1038/s41423-018-0027-x
38. Dong ZY, Zhong WZ, Zhang XC, Su J, Xie Z, Liu SY, et al. Potential predictive value of TP53 and KRAS mutation status for response to PD-1 blockade immunotherapy in lung adenocarcinoma. Clin Cancer Res. 2017;23(12):3012–24. doi:10.1158/1078-0432.CCR-16-2554
39. Marinelli D, Mazzotta M, Scalera S, Terrenato I, Sperati F, D'Ambrosio L, et al. KEAP1-driven co-mutations in lung adenocarcinoma unresponsive to immunotherapy despite high tumor mutational burden. Ann Oncol. 2020;31(12):1746–54. doi:10.1016/j.annonc.2020.08.2105
40. Hellmann MD, Ciuleanu TE, Pluzanski A, Lee JS, Otterson GA, Audigier-Valette C, et al. Nivolumab plus ipilimumab in lung cancer with a high tumor mutational burden. N Engl J Med. 2018;378(22):2093–104. doi:10.1056/NEJMoa1801946
41. Oh JH, Jang SJ, Kim J, Sohn I, Lee JY, Cho EJ, et al. Spontaneous mutations in the single TTN gene represent high tumor mutation burden. NPJ Genom Med. 2020;5(1):33. doi:10.1038/s41525-019-0107-6
42. Kanwal M, Ding XJ, Song X, Zhou GB, Cao Y. MUC16 overexpression induced by gene mutations promotes lung cancer cell growth and invasion. Oncotarget. 2018;9(15):12226–39. doi:10.18632/oncotarget.24203
43. Tomasini P, Walia P, Labbe C, Jao K, Leighl NB. Targeting the KRAS pathway in non-small cell lung cancer. Oncologist. 2016;21(12):1450–60. doi:10.1634/theoncologist.2015-0084